Co-incorporated $NiV_2O_6/Ni(HCO_3)_2$ nanoflake arrays grown on nickel foam for high-performance supercapacitor

Shaolei Zhao, Keyu Tao and Yun Gong*

Department of Applied Chemistry, College of Chemistry and Chemical Engineering, Chongqing University, Chongqing 401331, P. R. China Tel: +86-023-65678932 E-mail: gongyun7211@cqu.edu.cn

Electrochemical measurements

Due to the mass loss of the Ni foam before and after the hydrothermal synthesis, the specific capacity of the as-obtained sample is evaluated by areal capacity. The areal capacity C_A (mAh cm^{-2}) or C_A' (F cm^{-2}) of the prepared sample can be calculated by using the equations:

$C_A = I\Delta t/(3.6S)$ and $C_A' = I\Delta t/(S\Delta V)$ (**1**)

where 'I' is the discharge current (A), 'Δt' is the discharge time (s), 'S' is the geometrical area of the active material on Ni foam (cm^2), and 'ΔV' represents the potential window (V).

An asymmetric supercapacitor (ASC) device was assembled in 2 M KOH solution for the two-electrode measurements, in which the obtained Co-incorporated $NiV_2O_6/Ni(HCO_3)_2$/NF was utilized as positive electrode, and the negative electrode of activated carbon (AC) was prepared as follows: 90 wt % activated carbon (AC) and 10 wt % polyvinylidene fluoride (PVDF) were mixed in N-methylpyrrolidone (NMP), then the resulting slurry was then coated onto a piece of nickel foam (1 cm × 1 cm) and dried at 80 °C in an oven overnight. The loading of the activated carbon (AC) is calculated based on the charge balance: $S_+C_{A+} = S_-C_{A-}$, where S_+/C_{A+} and S_-/C_{A-} refer to the geometrical area (cm^{-2}) and areal specific capacity (mAh cm^{-2}) of the positive and negative electrodes, respectively. The specific capacity of the ASC device was calculated based on equation **1**, in which S represents the geometrical area (cm^2) of positive and negative electrodes. The energy density (mWh cm^{-2}), power density P (mW cm^{-2}) of the device was obtained using equations **2** and **3**, respectively:

$E = \int IV(t)dt/(3.6S)$ (**2**)

$P = 3600E/\Delta t$ (**3**)

where 'V (t)' is discharge voltage. Coulomb efficiency η (%) of the device was calculated using equation **4**:

$\eta = \Delta t/\Delta t_c$ (**4**)

where Δt_c is the charge time (s).

Table S1 The names of the samples synthesized under different conditions.

	$Co(NO_3)_2$ (mmol)	Na_3VO_4 (mmol)	urea (mmol)	Solvent
S-0.25-20	0.25	0.25	5	H_2O (10 mL)
S-0.25-15	0.25	0.25	3.75	H_2O (10 mL)
S-0.25-10	0.25	0.25	2.5	H_2O (10 mL)
S-0.5-20	0.5	0.5	10	H_2O (10 mL)
S-0.1-20	0.1	0.1	2	H_2O (10 mL)
S-0.25-20-EW	0.25	0.25	5	H_2O /ethanol (5 mL/5 mL)

Co-incorporated $Ni(HCO_3)_2$	0.25	/	5	H_2O (10 mL)
No product	/	0.25	5	H_2O (10 mL)

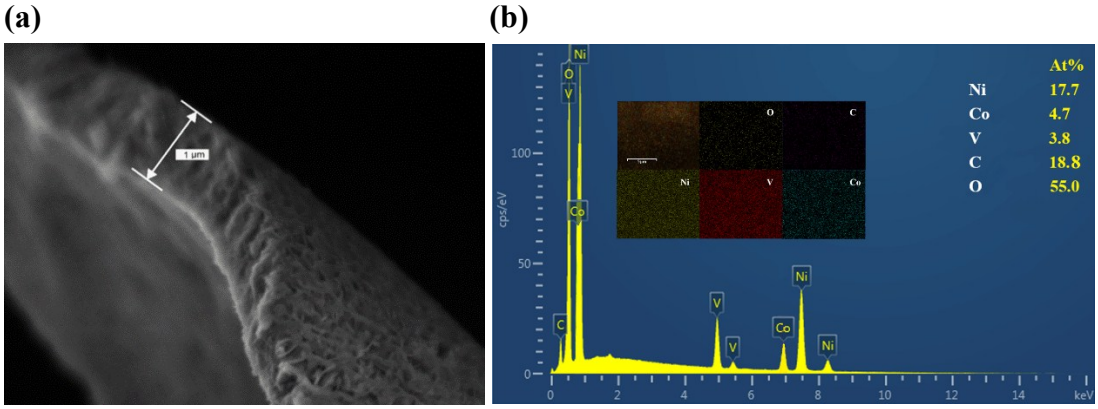

Fig. S1 SEM image (a) and EDS spectrum (inset: elemental mapping images) (**b**) of the sample S-0.25-20.

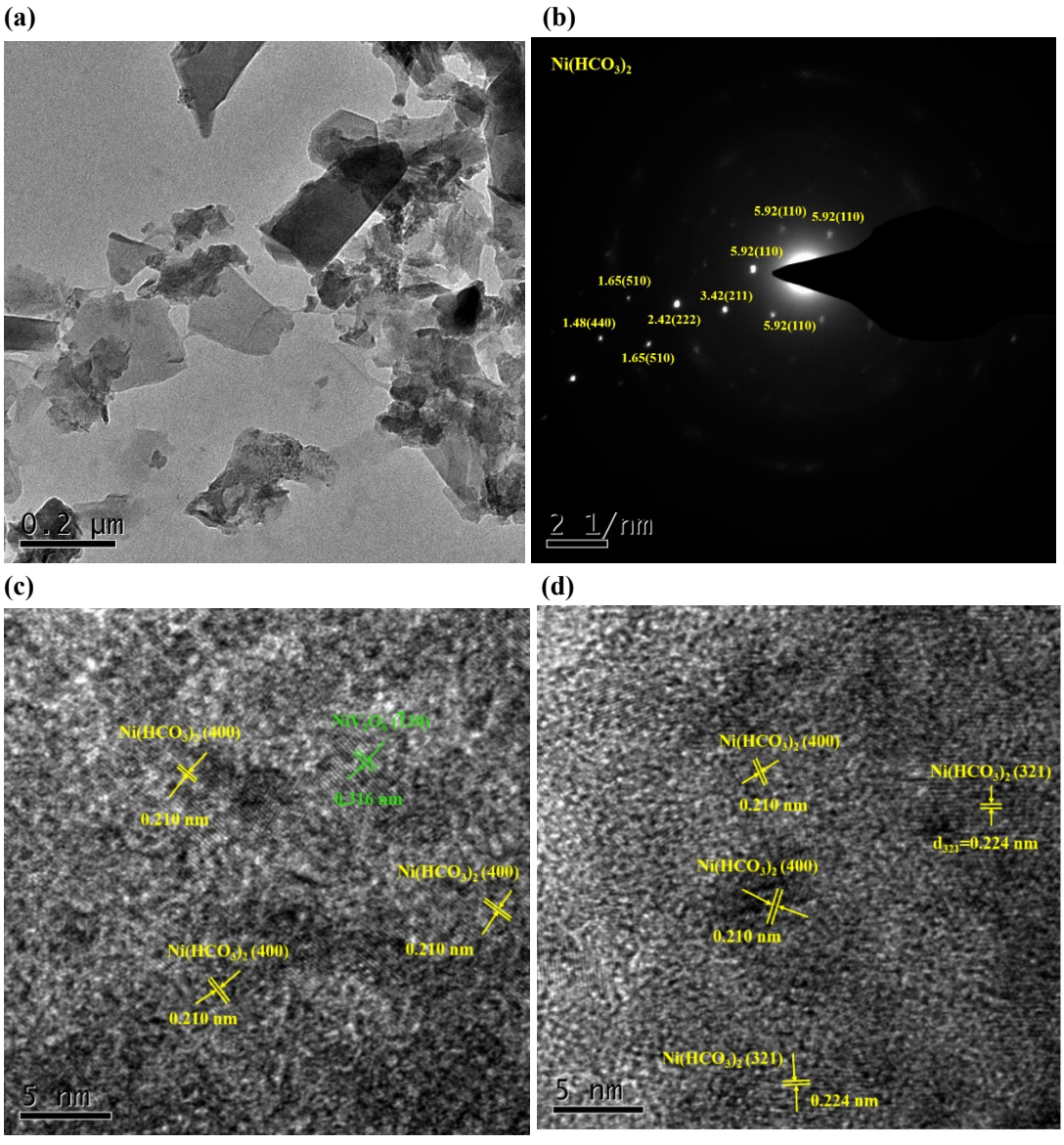

Fig. S2 TEM (**a**); SAED (**b**) and HRTEM (**c, d**) images of the Co-incorporated $NiV_2O_6/Ni(HCO_3)_2$/NF, S-0.25-20.

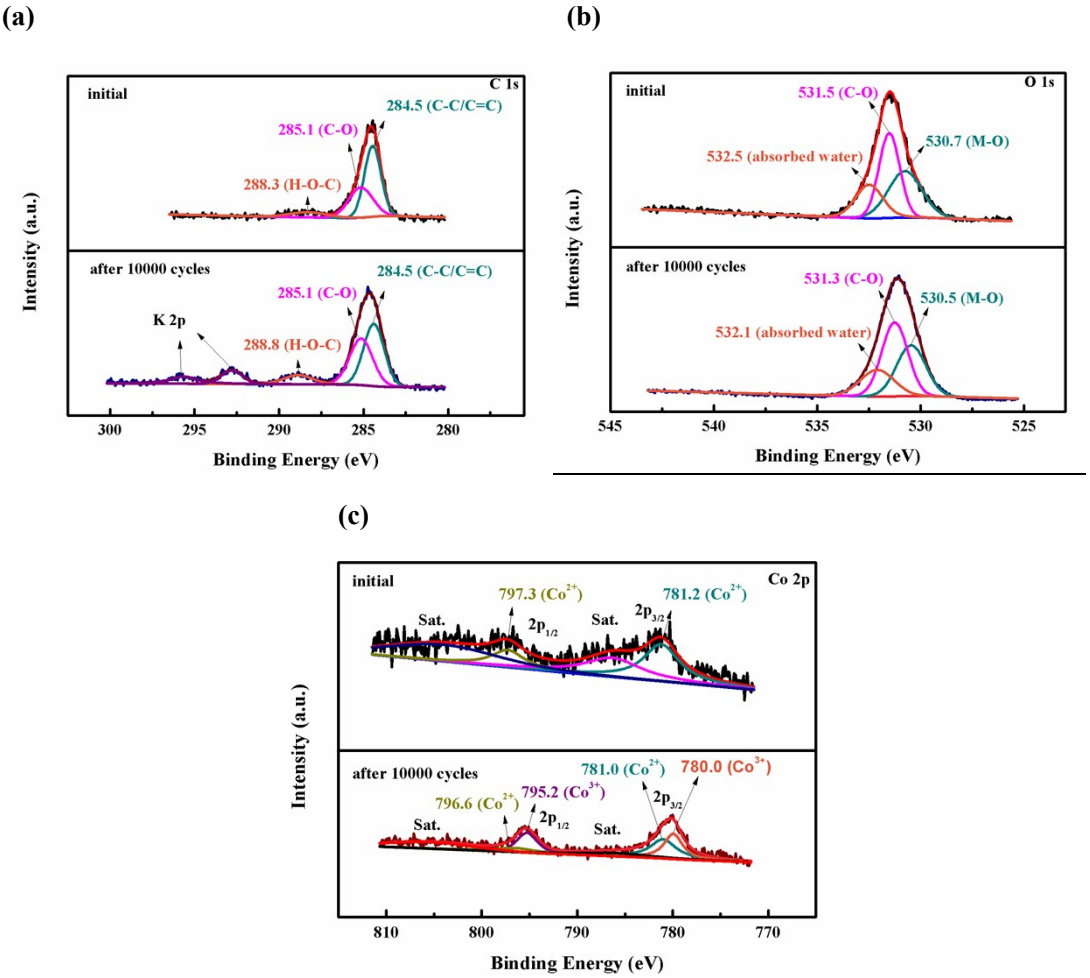

Fig. S3 XPS of C1s (**a**), O1s (**b**), and Co 2p (**c**) of the Co-incorporated $NiV_2O_6/Ni(HCO_3)_2$/NF, S-0.25-20 before (above) and after 10000 GCD cycles (below).

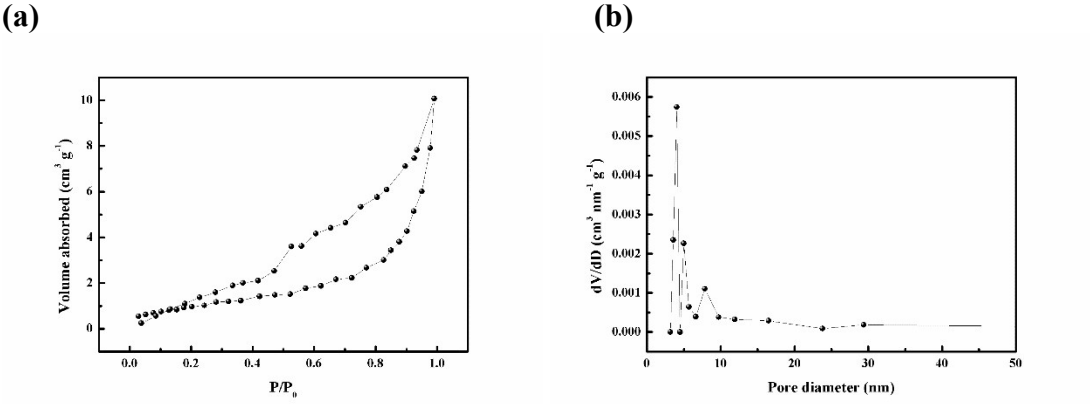

Fig. S4 Nitrogen adsorption/desorption isotherms (**a**) and the pore-size distribution curve of the Co-incorporated $NiV_2O_6/Ni(HCO_3)_2$/NF, S-0.25-20 (**b**).

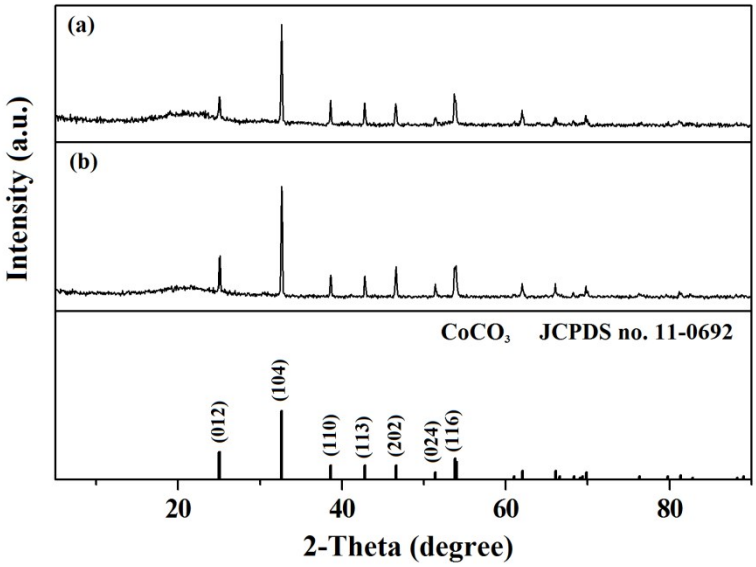

Fig. S5 The XRD patterns of the precipitations in the autoclave and the standard profile: in the preparation of S-0.25-20 (**a**) and synthesized in the absence of Na_3VO_4 (**b**).

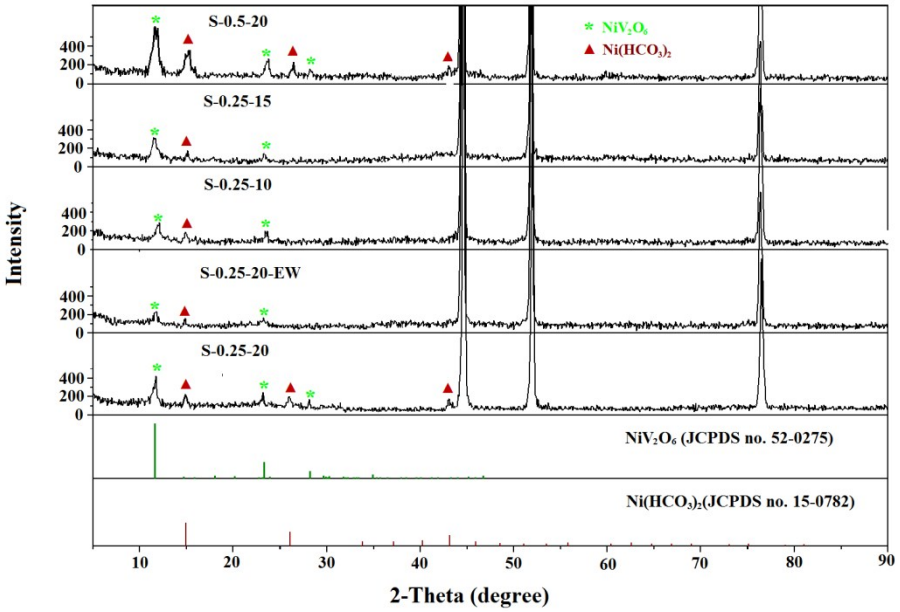

Fig. S6 The XRD patterns of S-0.25-10, S-0.25-15, S-0.5-20 and the sample synthesized in ethanol/H_2O (1: 1) mixed solvent in comparison with that of S-0.25-20.

(a)

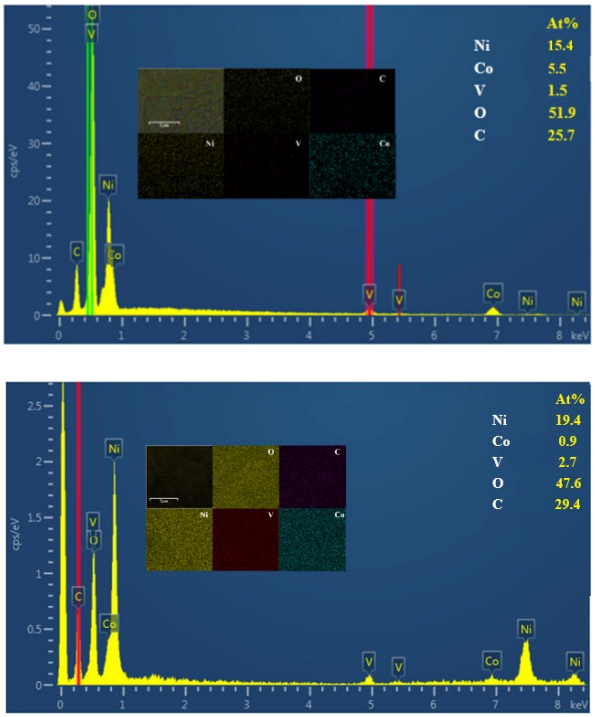

(b)

Fig. S7 EDS and elemental mapping images (inset) for S-0.25-10 (**a**) and S-0.25-15 (**b**).

(a) **(b)**

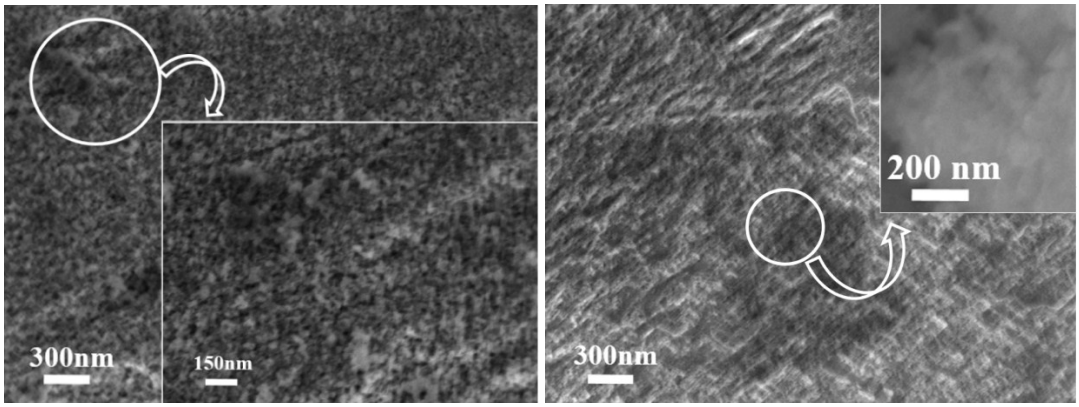

Fig. S8 SEM images for S-0.25-10 (**a**) and S-0.25-15 (**b**).

(a) **(b)**

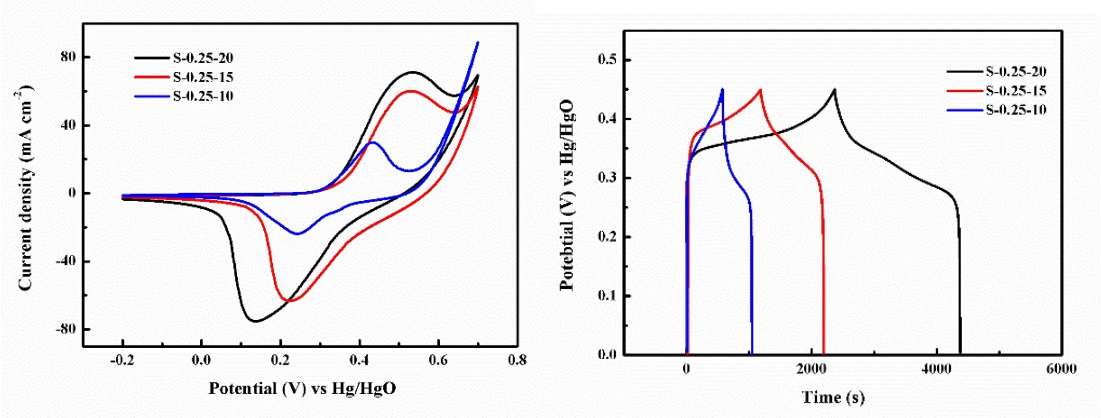

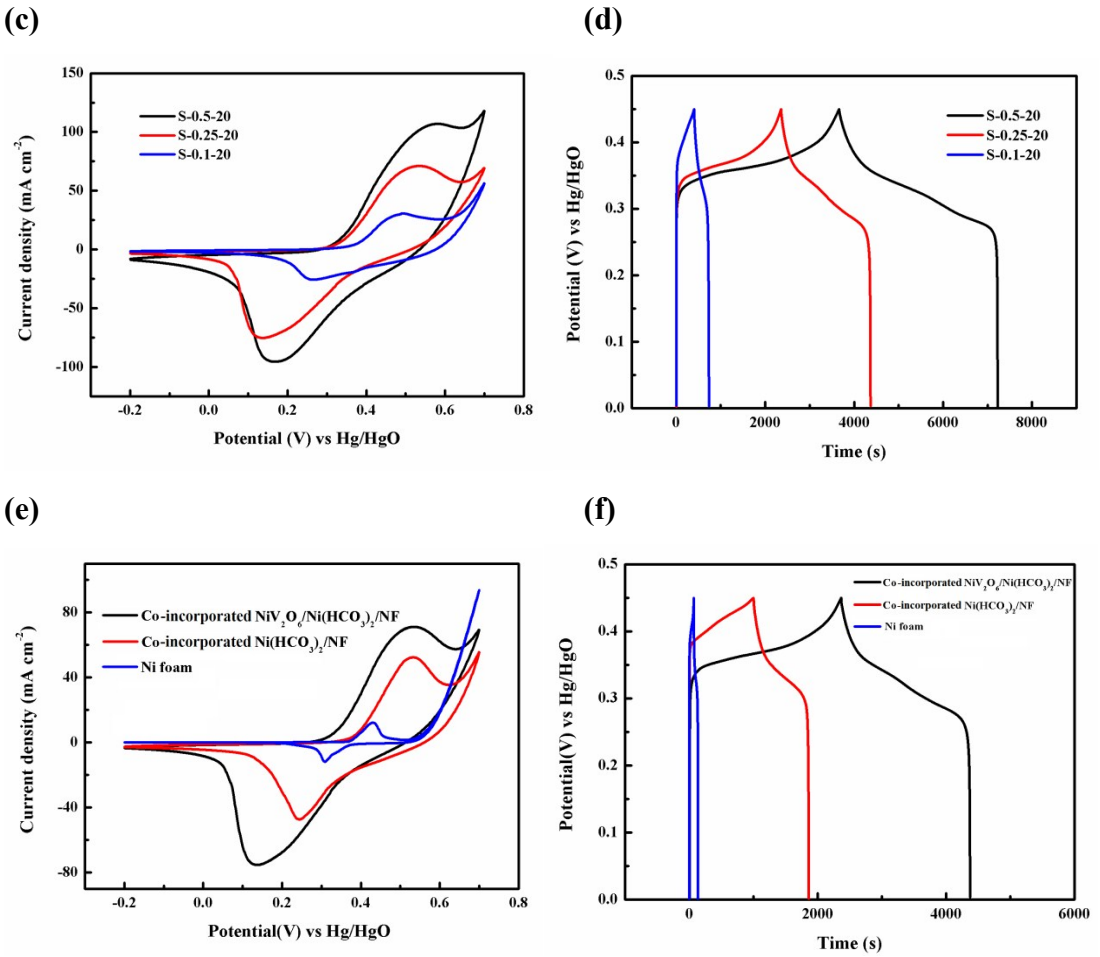

Fig. S9 CVs at 10 mV s^{-1} and GCD curves at 1 mA cm^{-2} for S-0.25-10, S-0.25-15 (**a, b**); S-0.5-20, S-0.1-20 (**c, d**) and the Co-incorporated $Ni(HCO_3)_2$/NF (**e, f**) in comparison with S-0.25-20.

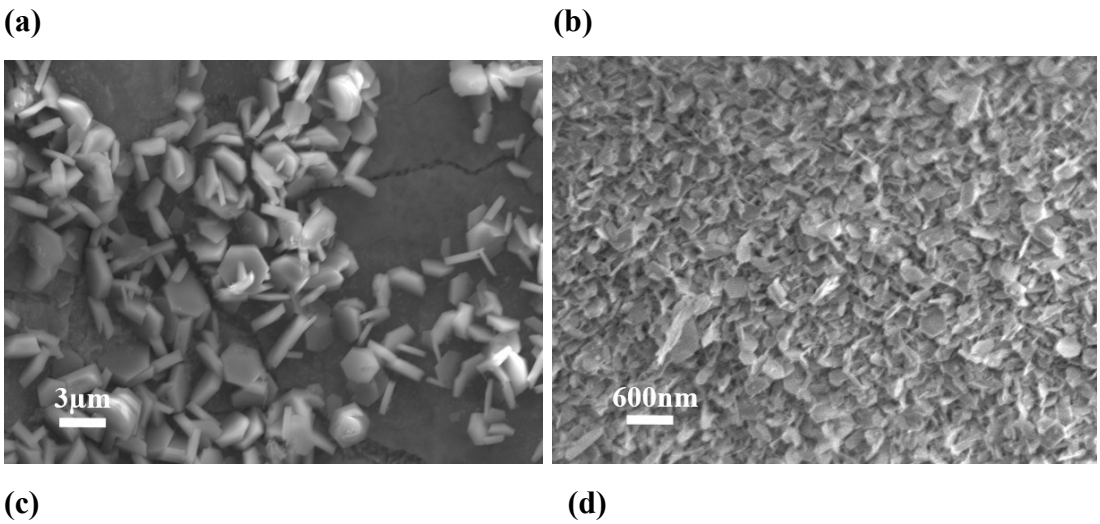

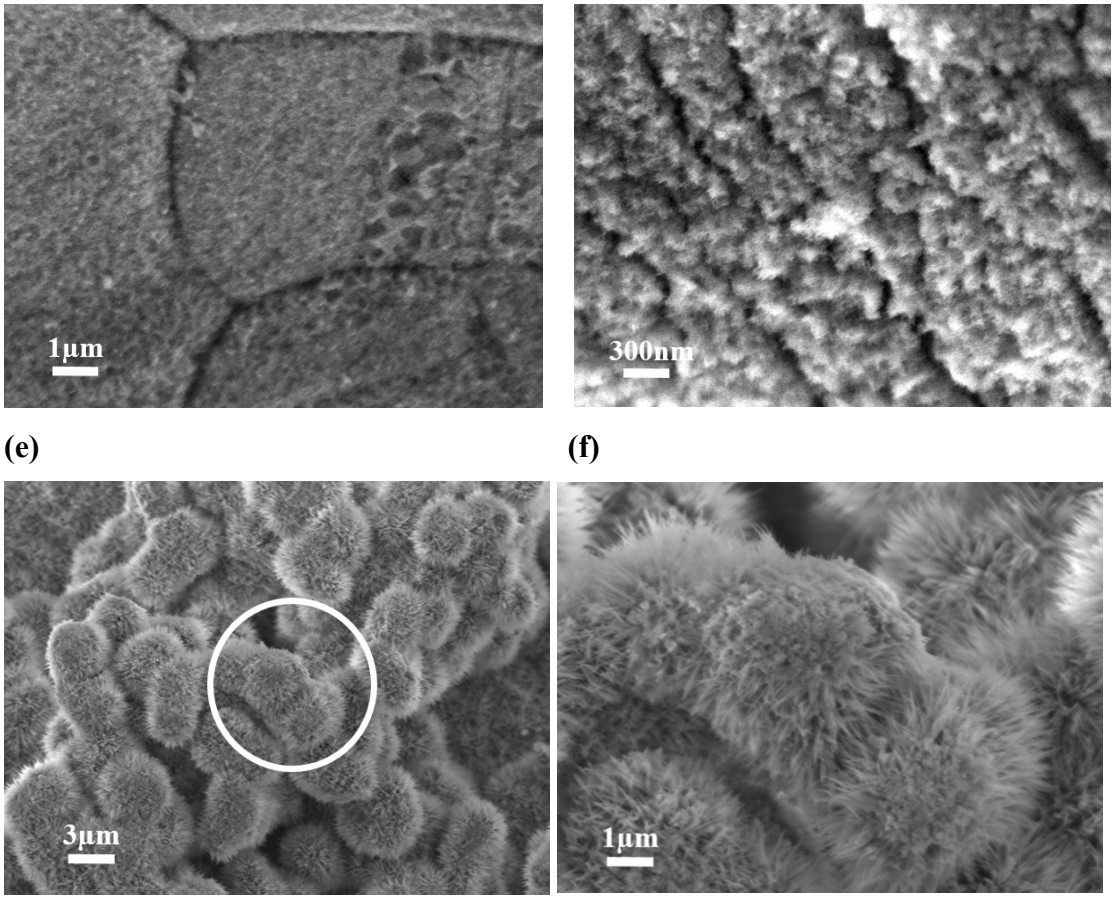

Fig. S10 SEM images for S-0.5-20 (**a, b**), S-0.1-20 (**c, d**) and Co-incorporated $Ni(HCO_3)_2$/NF synthesized in the absence of Na_3VO_4 at different magnifications (**e**, **f**).

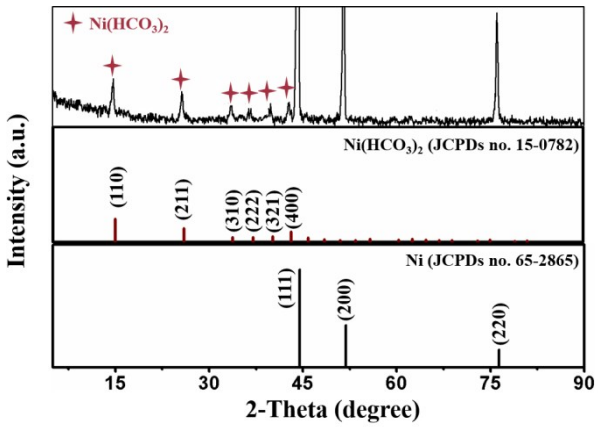

Fig. S11 The XRD pattern of the sample grown on Ni foam synthesized in the absence of Na_3VO_4 and the standard profiles.

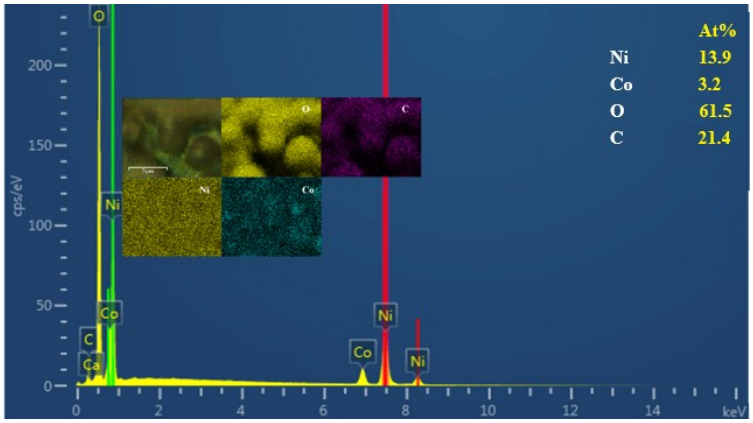

Fig. S12 EDS and elemental mapping images (inset) of the Co-incorporated $Ni(HCO_3)_2$/NF.

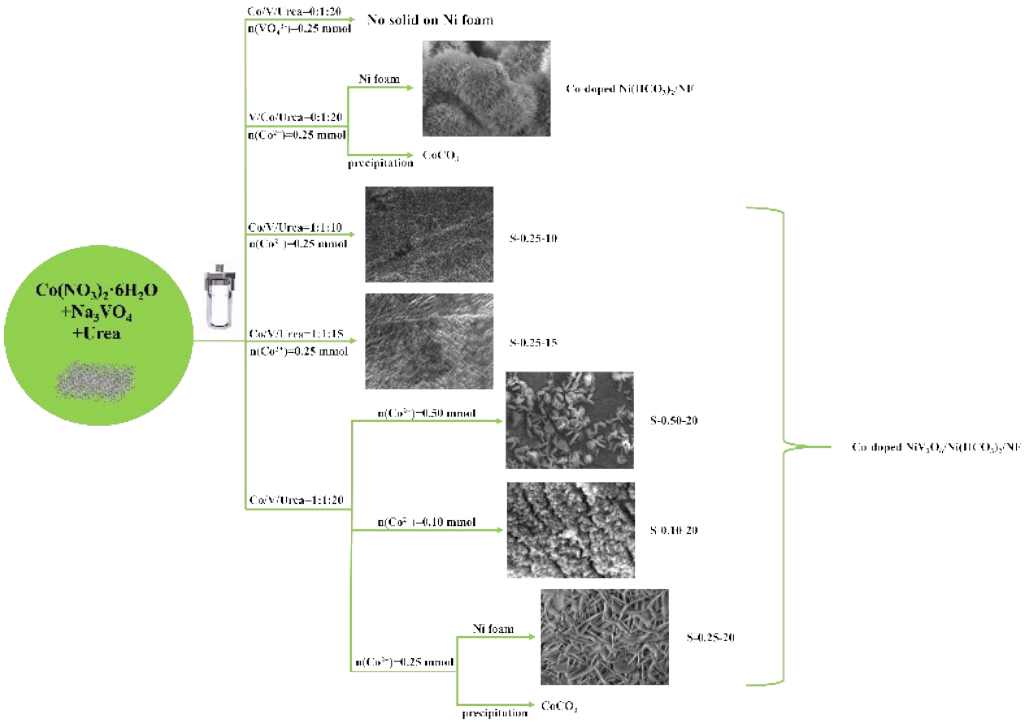

Scheme S1 The hydrothermal synthetic conditions for Co-incorporated $NiV_2O_6/Ni(HCO_3)_2$/NF and Co-incorporated $Ni(HCO_3)_2$/NF.

Table S2 The comparison of the capacity, energy density, power density and capacity retention.

	Electrode	Specific capacity	Energy density	Electrolyte	Capacity retention	Ref.
1	$Ni_3V_2O_8/Co_3V_2O_8$	5.13 F cm^{-2} at 2.5 mA cm^{-2}	——	2 M KOH	85.1% (1000 cycles at 25 mA cm^{-2})	10
2	$Co_3V_2O_8$	0.42 mAh cm^{-2} at 0.84 mA cm^{-2}	——	1 M $LiPF_6$ in EC:DMC (1:1 in volume)	——	11
3	CoV_2O_6	0.669 F cm^{-2} at 3 mA cm^{-}	——	2 M KOH	123.3% (15000 cycles	13

		^{2}			at 15 mA cm^{-2})	
4	NiV_2O_6/C	0.75 F cm^{-2} at 0.5 mA cm^{-2}	0.032 m Wh cm^{-2} at 0.375 mW cm^{-2}	2 M KOH	77.8% (12000 cycles at 2 mA cm^{-2})	14
5	$MnCO_3$ QDs/Ni(HCO$_3$)$_2$-$MnCO_3$	3.55 F cm^{-2} at 6 mA cm^{-2}	0.116 m Wh cm^{-2} at 1.8 mW cm^{-2}	1 M KOH	85.5% (5000 cycles at 30 mA cm^{-2})	15
6	$Ni(OH)_2$/ $Ni(HCO_3)_2$	3.4 F cm^{-2} at 10 mA cm^{-2}	——	6 M KOH	55% (3750 cycles at 10 mA cm^{-2})	16
7	$Ni_2(CO_3)$ $(OH)_2$	6.2 F cm^{-2} at 2.65 mA cm^{-2}	——	3 M KOH	——	17
8	$Ni_3V_2O_8$ @GO	0.59 F cm^{-2} at 10 mA cm^{-2}	0.035 mWh cm^{-2} at 0.5 mW cm^{-2}	6 M KOH	95% (1500 cycles at 5 A g^{-1})	28
9	C@V_2O_5	0.45 F cm^{-2} at 0.5 mA cm^{-2}	0.009 mWh cm^{-2} at 0.170 mW cm^{-2}	0.5 M K_2SO_4	——	29
10	$Ni_{0.75}Co_{0.25}$ $(CO_3)_{0.125}$ $(OH)_2$	1.18 F cm^{-2} at 5 mA cm^{-2}	0.22 mWh cm^{-2} at 2.3 mW cm^{-2}	1 M KOH	98.5% (1000 cycles at 3 A g^{-1})	30
11	$Ni(HCO_3)_2$@ $(Cu_{0.2}Ni_{0.8})O$	7 F cm^{-2} at 3.5 mA cm^{-2}	0.185 mWh cm^{-2} at 0.56 mW cm^{-2}	6 M KOH	74.42% (3000 cycles at 5 A g^{-1})	31
12	$CoWO_4$@ $NiWO_4$	2.03 F cm^{-2}at 3 mA cm^{-2}	0.035 mWh cm^{-2} at 3.27 mW cm^{-2}	1 M KOH	80% (2000 cycles at 5 A g^{-1})	32
13	Co-incorporated NiV_2O_6/ $Ni(HCO_3)_2$	4.48 F cm^{-2} (0.56 mAh cm^{-2}) at 1 mA cm^{-2}	0.533 m Wh cm^{-2} at 0.232 mW cm^{-2}	2 M KOH	106.2% (10000 cycles at 100 mA cm^{-2})	This work

Table S3 Parameters of the simulated equivalent circuit for the Co-incorporated $NiV_2O_6/Ni(HCO_3)_2$/NF, S-0.25-20 before and after 10000 GCD cycles.

	R_s/Ω cm^{-2}	Q	R_{ct}/Ω cm^{-2}	C/F cm^{-2}	R_1/Ω cm^{-2}
Before 10000 GCD cycles	1.093	0.0061	2.202	0.001	7336
After 10000 GCD cycles	1.334	0.0020	4.389	0.003	2072

(a) **(b)**

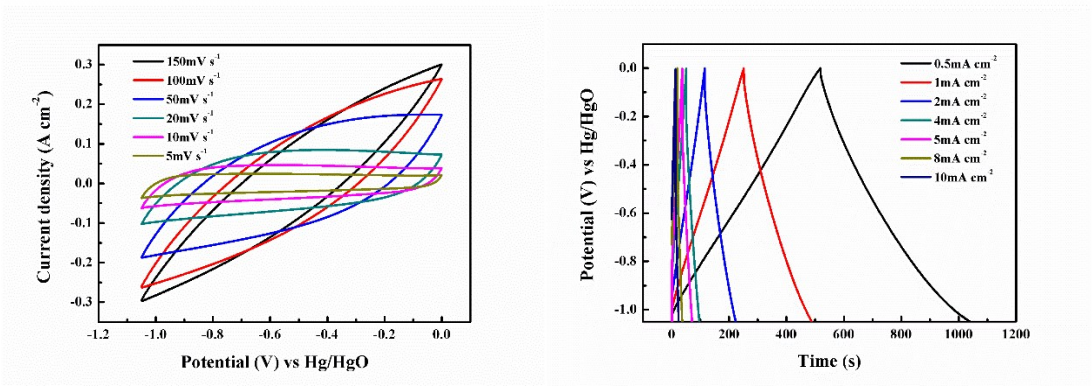

(c)

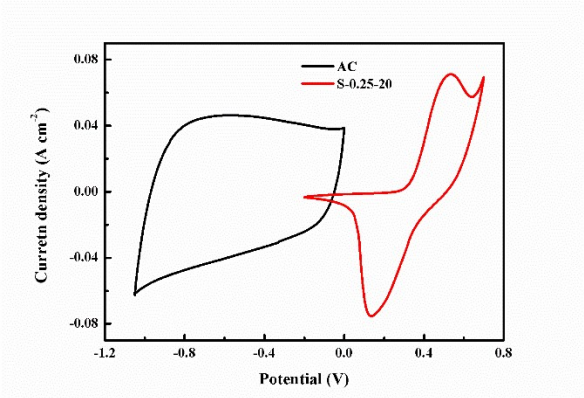

Fig. S13 CVs at different scan rates (**a**) and GCD curves at different current densities of AC (**b**); The comparative CV curves of S-0.25-20 and AC at the same scan rate of 20 mV s^{-1}.

(a)

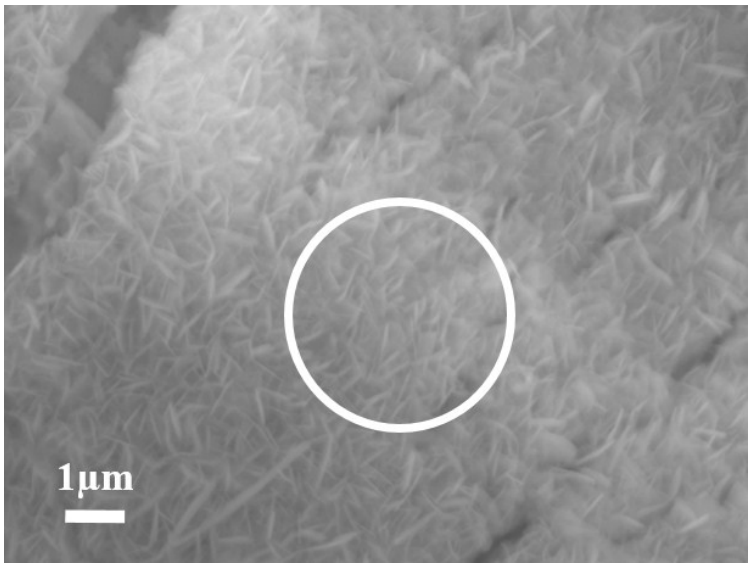

(b)

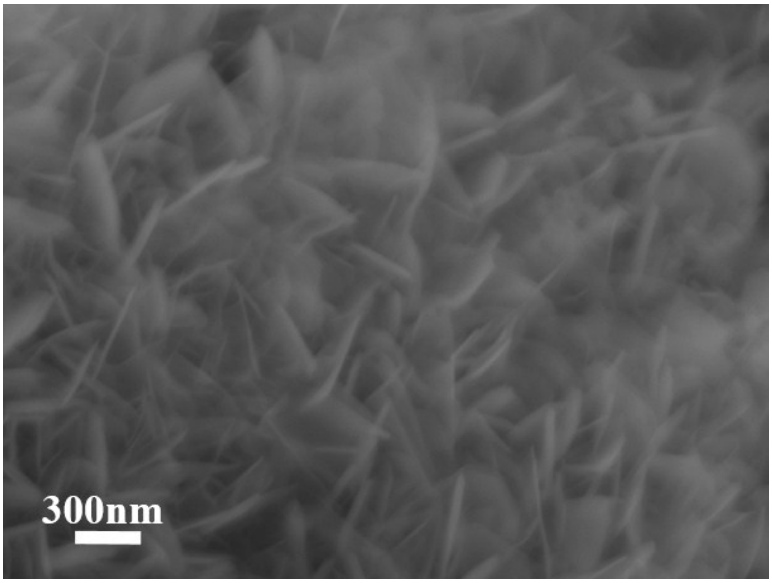

(c)

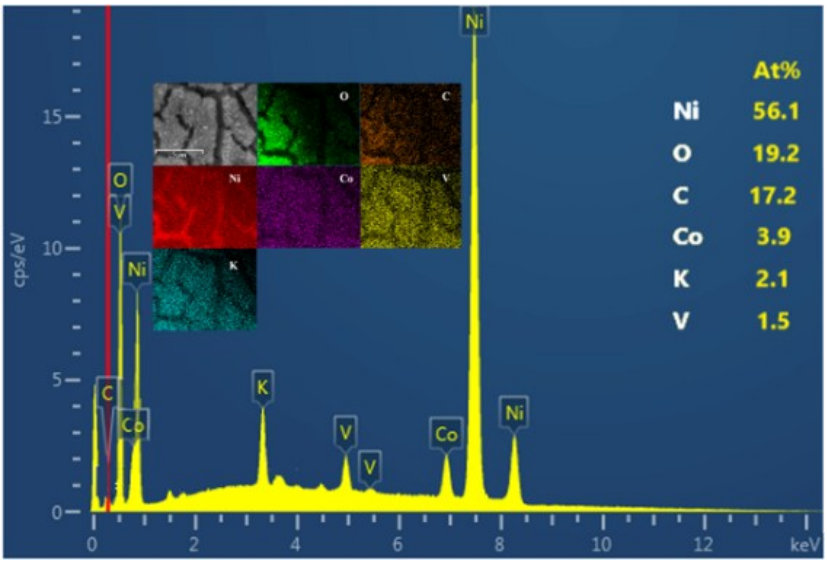

Fig. S14 SEM (**a, b**) and EDS as well as elemental mapping images (inset) (**c**) for S-0.25-20 after 10000 GCD cycles.